Reliability – Based Design of Precast Buildings

M. Kalousková, E. Novotná, J. Šejnoha

We present a numerical analysis of a precast structure regarding random properties of the material characteristics of joints, as well as the random character of loading, especially due to temperature impact. Using FEM we compare some of our results with a deterministic nonlinear solution.

Keywords: reliability, precast buildings, joints of panels, two-parameter subgrade, reliability index.

1 Introduction

A number of numerical methods may be applied when estimating the bearing capacity of existing as well as planned buildings with random properties of structural elements, especially of vertical and horizontal joints.

At present, probabilistic methods can be broadly classified into two major categories – methods using a statistical approach and methods using a nonstatistical approach [1]. Statistical methods are based on simulation. The direct Monte Carlo method and the Latin Hypercube Sampling (LHS) technique are fairly known, as well as improved simulation methods known as "Importance Sampling" and "Adaptive Sampling". Nonstatistical methods include numerical integration, the method of second order moments and the probabilistic finite element method.

The horizontal and vertical joints of precast buildings and their properties are structural elements of the utmost importance. Calculations based on statistical methods and taking into account the random material properties of joints and panels, as well as the random properties of loading, especially due to temperature impact, are rather complicated and time consuming. That is why a different approach using reliability index β is preferred to the direct determination of failure probability. It is well known that very low values of β are attained ($\beta \leq 2$) when deterioration of the joint due to an extreme inelastic deformation and/or due to a certain type of cyclic loading is developed to such an extent that the consecutive static stiffness approaches its residual value. A typical loading path of a reinforced vertical joint published in [5] is displayed in Fig. 1.

Based on this observation, the proposed procedure is as follows. Index β is determined using the second order reliability method. In the parts of joints where values of β are rather low, the initial stiffnesses of the joints are reduced to

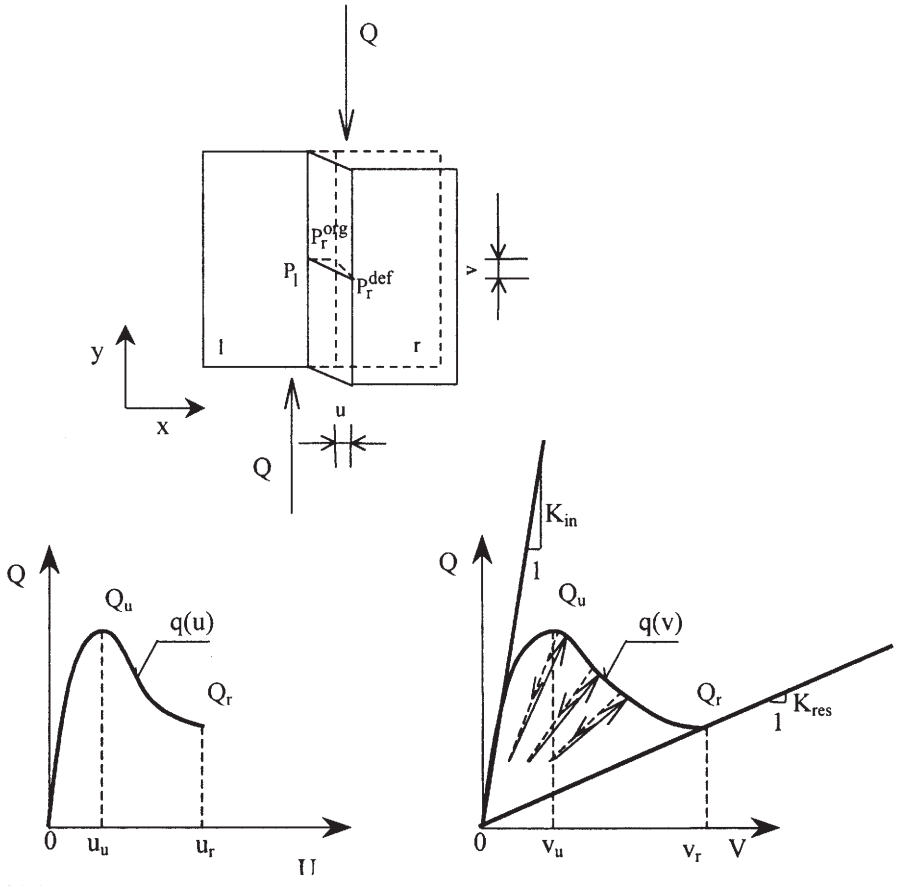

Fig. 1: Loading paths for a vertical joint

their residual values. The aim of this paper is to demonstrate that

- this simple algorithm, which does not require an examination of the whole loading path from Fig. 1, makes it possible to describe the propagation of the deteriorated regions of joints,
- the image of these regions is similar to that obtained by the well-tried finite element deterministic solutions.

2 Reliability analysis of joints

Probabilistic analysis is carried out using the NASREL (Numerical Analysis of Structures for Reliability) code. NASREL is the high performance finite element NASCOM (Numerical Analysis of Structures and Combined Objects) code integrated with COMREL (Componental Reliability Analysis). The second order reliability method SORM is used to determine reliability index b at selected points of the joints. Under the assumption that a failure domain $g(\mathbf{u}) \le 0$, $\mathbf{u}$ being the normalized basic uncertainty variables, is twice differentiable, the failure surface $g(\mathbf{u}) = 0$ in the vicinity of the critical point $\mathbf{u}^*$ with the distance $\beta = \|\mathbf{u}^*\|$ to the origin is approximated by its supporting hyperparaboloid. Expanding the function g into the Taylor series up to the second order terms and introducing certain orthogonal transformations, the failure surface can be written as:

$$\{g(\mathbf{U}) \le 0\} \approx \left\{ U_n \le -\beta + \frac{1}{2}\sum_{i=1}^{n-1} \kappa_i U_i^2 \right\}. \qquad (1)$$

Parameters, κ_i, $i = 1, 2, \ldots, n$, stand for the second order derivatives in the principal directions of the failure surface. An expression for the failure probability can be found in [6] in this form

$$P[g(\mathbf{U}) \le 0] \approx \Phi(-\beta)\prod_{i=1}^{n-1}(1-\beta\kappa_i)^{-1/2}, \qquad (2)$$

where Φ is the Laplace function.

The Rackwitz/Fiessler optimization procedure is used to find the design point.

3 Model of a precast building

The FEM code NASCOM is called when analyzing the state of stress in walls and joints of a precast structure. In this paper, 3D elements have been used for panels and joints, beam elements to model a continuous footing, and beam and truss elements for the equivalent subgrade structures.

A 3D Coulomb condition describes *the failure envelope* in joints [3] as

$$\sigma_i - \sigma_j \cot g^2\left(\frac{\pi}{4} - \frac{\varphi}{2}\right) = \sigma_{\mathrm{red}}, \quad i \ne j,\ i = 1, 2, 3,\ j = 1, 2, 3 \qquad (3)$$

$$\sigma_{\mathrm{red}} = 2c\frac{\cos\varphi}{1-\sin\varphi}, \qquad (4)$$

where

σ_i, σ_j	principal stresses,
c	cohesion coefficient
φ	friction angle.

If $\sigma_1 > \sigma_2 > \sigma_3$, condition (3) reduces to

$$\sigma_1 - \sigma_3 \cot g^2\left(\frac{\pi}{4} - \frac{\varphi}{2}\right) = \sigma_{\mathrm{red}}. \qquad (5)$$

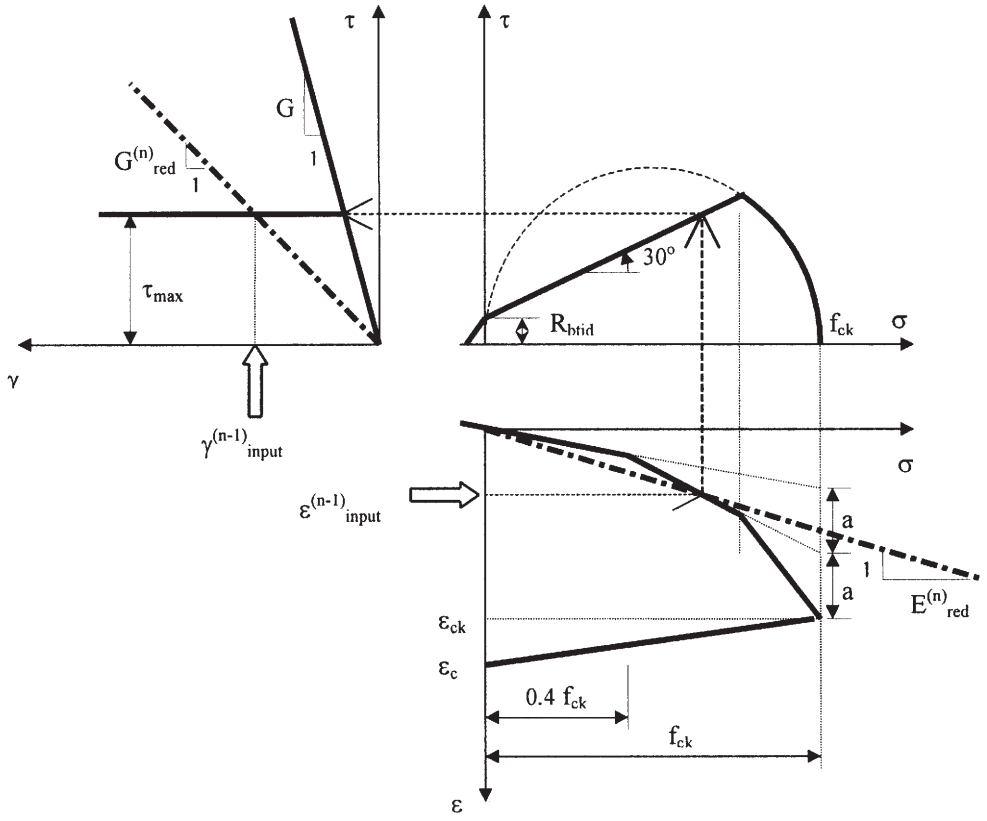

Fig. 2: Interaction diagram for a joint

Regarding the fact that the material of joints is plastically anisotropic, condition (5) can be written as [4]

$$\eta\sigma_1 - \sigma_3 = 2c\sqrt{\eta}, \tag{6}$$

where

$\eta = \frac{R_c}{R_i}$ ratio of the strength in compression to the strength in tension.

The following three loadings are combined – the dead load, the loading transferred from the ceiling panels, and the temperature. All of these are supposed to be randomly distributed.

In the deterministic solution the 2D finite elements are preferred to the 3D formulation discussed above. Fig. 2 shows a material model describing the interaction between the shear and normal stresses. Diagram $\tau - \sigma$ has been derived from experimental results for a layer of lower strength [2]. The model is characterized by the following parameters – the characteristic strength f_{ck}, the ultimate strains ε_{ck} and ε_c. The proportional limit σ_e is equal to 0.4 f_{ck}. The determination of reduced stiffnesses E_{red}, G_{red} at the n-th iteration step is based on the assumption that strains $\varepsilon^{(n-1)}$ and $\gamma^{(n-1)}$ from the preceding iteration step are known. The algorithm starts by determining the reduced stiffness E_{red}. Next, the corresponding ultimate shear strength of the joint τ_{max} is determined. Finally, G_{red} is assigned to the known $\gamma^{(n-1)}$. This algorithm is implemented in the finite element code FEAT, where contact elements are used to model the joints. For more details, see [2].

4 Model of a subgrade

The proposed analysis of a precast structure takes into account the structure-subgrade interaction. A straightforward way to solve this problem by the NASCOM code is to use 3D elements for both the structure and subsoil. An alternative and more effective approach is based on the Winkler – Pasternak model with two parameters, which is not implemented in the NASCOM code. This model is described in a concise manner in what follows. The stiffness of the subgrade is replaced by the stiffness of an equivalent construction composed of truss and beam elements, as shown in Fig. 3.

As for the model of the subgrade, noninteracting foundation structures are considered [1]. Three basic types of elements are used (Fig. 4) and the deformation of each of them is given by the vertical displacements of end-points 1 and 2.

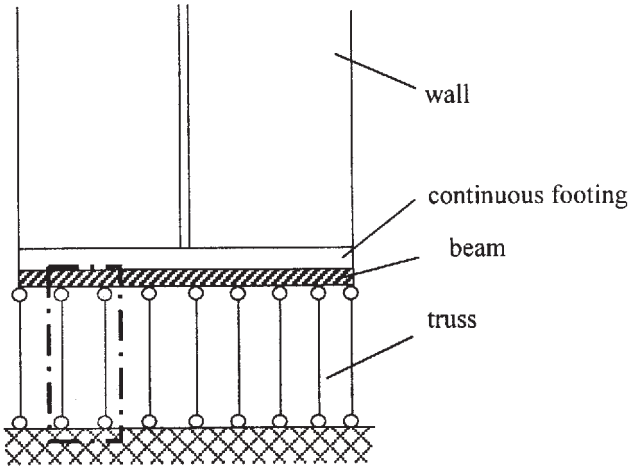

Fig. 3: Beam and truss construction

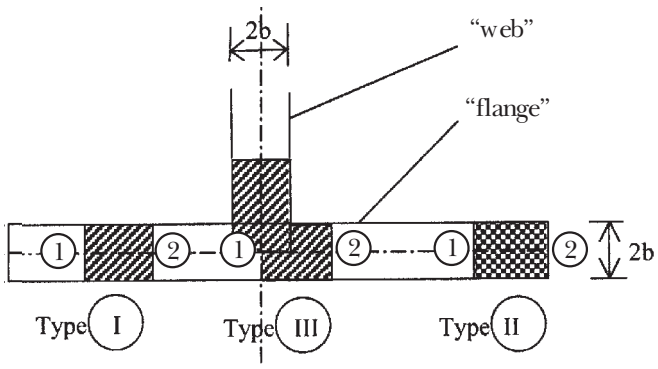

Fig. 4: Basic types of subgrade elements

a) ***Inner element I***

The stiffness matrix of the subgrade element is expressed [1] as

$$\left[K^{\mathrm{I}}_{\mathrm{WP}}\right] = \begin{bmatrix} \frac{2b\ell}{3}C_1^* + \frac{2b}{\ell}C_2^* & \frac{b\ell}{3}C_1^* - \frac{2b}{\ell}C_2^* \\ \frac{b\ell}{3}C_1^* - \frac{2b}{\ell}C_2^* & \frac{2b\ell}{3}C_1^* + \frac{2b}{\ell}C_2^* \end{bmatrix}, \tag{7}$$

where $2b$ width of foundation

ℓ length of element

C_1, C_2 stiffness parameters of the Winkler-Pasternak model

C_1^*, C_2^* modified parameters defined as

$$C_1^* = C_1 + \frac{1}{b}\sqrt{C_1 C_2}\,,$$

$$C_2^* = C_2 + \frac{1}{2b}\sqrt{\frac{C_2^3}{C_1}}\,.$$

The corresponding stiffness matrix $[K_{\mathrm{BT}}]$ of the equivalent beam and truss element (see Fig. 5) is given by

$$[K_{\mathrm{BT}}]^{\mathrm{I}} = \begin{bmatrix} \frac{1}{2}\frac{E_{\mathrm{T}}A_{\mathrm{T}}}{h} + \frac{12E_{\mathrm{B}}I_{\mathrm{B}}}{\ell^3(1+2\kappa)} & -\frac{12E_{\mathrm{B}}I_{\mathrm{B}}}{\ell^3(1+2\kappa)} \\ -\frac{12E_{\mathrm{B}}I_{\mathrm{B}}}{\ell^3(1+2\kappa)} & \frac{1}{2}\frac{E_{\mathrm{T}}A_{\mathrm{T}}}{h} + \frac{12E_{\mathrm{B}}I_{\mathrm{B}}}{\ell^3(1+2\kappa)} \end{bmatrix}, \tag{8}$$

where $A_{\mathrm{T}}, A_{\mathrm{B}}$ cross-section areas of truss and beam, respectively

$E_{\mathrm{T}}, E_{\mathrm{B}}$ Young moduli of truss and beam, respectively

ℓ length of beam element

h length of truss

I_{B} moment of inertia of the beam cross section

$\kappa = \frac{6E_{\mathrm{B}}I_{\mathrm{B}}}{kGA_{\mathrm{B}}\ell^2}$ coefficient expressing the influence of shear.

Comparing the equivalent stiffness matrices (7) and (8) gives

$$\frac{1}{2}\frac{E_{\mathrm{T}}A_{\mathrm{T}}}{h} + \frac{12E_{\mathrm{B}}I_{\mathrm{B}}}{\ell^3(1+2\kappa)} = \frac{2b\ell}{3}C_1^* + \frac{2b}{\ell}C_2^*, \tag{9}$$

$$\frac{12E_{\mathrm{N}}I_{\mathrm{N}}}{\ell^3(1+2\kappa)} = \frac{b\ell}{3}C_1^* - \frac{2b}{\ell}C_2^*. \tag{10}$$

The determination of the beam and truss characteristics is evident.

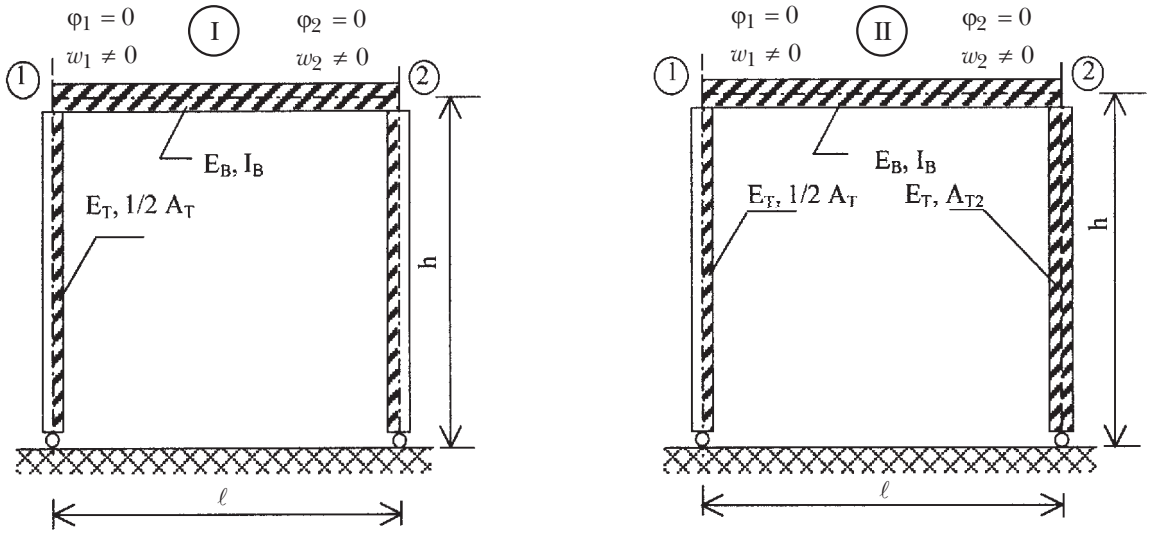

Fig. 5: Equivalent beam and truss construction – elements of types I, II

b) ***End – point element II***

The stiffness matrix of the subgrade element is obtained from (7) by adding a complementary matrix

$$[\Delta K_{\mathrm{WP}}]^{\mathrm{II}} = \begin{bmatrix} 0 & 0 \\ 0 & 2b\sqrt{C_1C_2} + \frac{3}{2}C_2 \end{bmatrix}. \tag{11}$$

c) ***Inner corner element III***

The interaction of the crossing beams cannot be neglected. Substituting the following expression for the displacement of the subgrade in the vicinity of the inner corner,

$$w(x,y) = W_0\left(e^{-\sqrt{\frac{C_1}{C_2}}x} + e^{-\sqrt{\frac{C_1}{C_2}}y} - e^{-\sqrt{\frac{C_1}{C_2}}x} \cdot e^{-\sqrt{\frac{C_1}{C_2}}y} \right),$$

into the principle of virtual displacements yields formulas for the shear forces q_x, q_y acting along the crossing beams (unit corner displacement W_0 is considered):

$$\begin{aligned} q_{\mathrm{x}} &= \sqrt{C_1C_2}\cdot\varphi(y) \\ q_{\mathrm{y}} &= \sqrt{C_1C_2}\cdot\varphi(x) \end{aligned}, \tag{12}$$

where

$$\varphi(y) = 1 - e^{-\sqrt{\frac{C_1}{C_2}}y} + \frac{3}{4}e^{-2\sqrt{\frac{C_1}{C_2}}y}. \tag{13}$$

For $y = 0$ or $x = 0$ we have

$$q_{\mathrm{x}} = q_{\mathrm{y}} = \frac{3}{4}\sqrt{C_1C_2}. \tag{14}$$

For $y = \ell_0$ or $x = \ell_0$ (ℓ_0 being length of the shear depression)

$$q_{\mathrm{x}} = q_{\mathrm{y}} = \sqrt{C_1C_2}. \tag{15}$$

Applying equations (12) through (15) to the elements in the vicinity of the inner corner (Fig. 6) yields

$$[K_{\mathrm{WP}}]^{\mathrm{III}} = \begin{bmatrix} k_{11} & k_{12} \\ k_{21} & k_{22} \end{bmatrix},$$

where for the "flange" shown in Fig. 6

$$k_{11}^{\mathrm{F}} = k_{22}^{\mathrm{F}} = \frac{2b\ell}{3}C_1 + \frac{2\ell}{3}\sqrt{C_1C_2}(\varphi(x_{\mathrm{s}})+1) + \frac{2b}{\ell}C_2^*, \tag{16}$$

$$k_{12}^{\mathrm{F}} = k_{21}^{\mathrm{F}} = \frac{b\ell}{3}C_1 + \frac{\ell}{3}\sqrt{C_1C_2}(\varphi(x_{\mathrm{s}})+1) - \frac{2b}{\ell}C_2^*, \tag{17}$$

and for the "web"

$$k_{11}^{\mathrm{W}} = k_{22}^{\mathrm{W}} = \frac{2b\ell}{3}C_1 + \frac{2\ell}{3}\sqrt{C_1C_2}\,\varphi(y_{\mathrm{s}}) + \frac{2b}{\ell}C_2^*, \tag{18}$$

$$k_{12}^{\mathrm{W}} = k_{21}^{\mathrm{W}} = \frac{b\ell}{3}C_1 + \frac{\ell}{3}\sqrt{C_1C_2}\,\varphi(y_{\mathrm{s}}) - \frac{2b}{\ell}C_2^*. \tag{19}$$

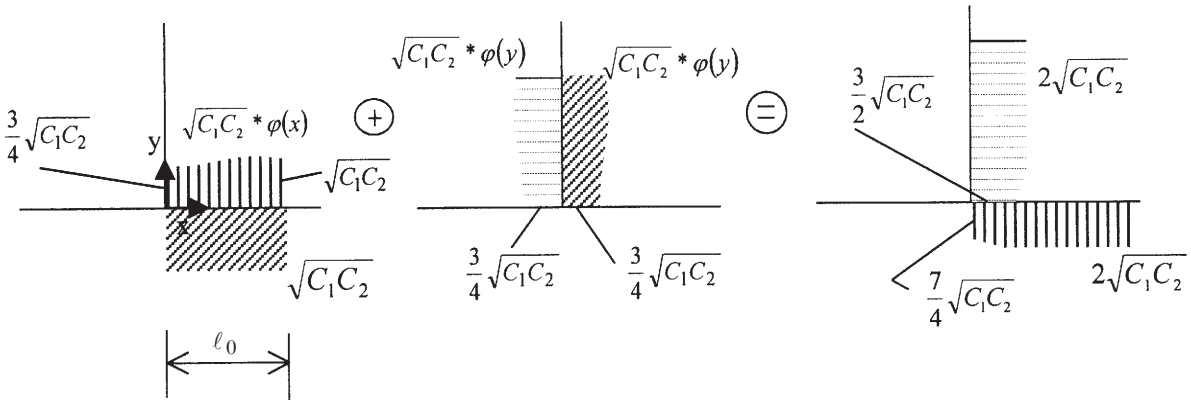

Fig. 6: Distribution of shear forces in the vicinity of the inner corner

5 Numerical example

Part of a seven-story precast building of type G57 was analysed (Fig. 7). The construction with the continuous footing lies on a sandy loam subgrade ($C_1 = 15$ MNm^{-3}, $C_2 = 5$ MNm^{-1}, $E_0 = 35$ MPa). The statistical properties of the basic variables applied to the reliability analysis are listed in Table 1. The aim of this paper is to demonstrate the propagation of deteriorated regions rather than to describe truthfully the random properties of the building. For simplicity, all variables except for the friction angle, which is a constant, are supposed to be normally distributed with the coefficient of variation 0.1. The temperature loading is caused by exposing one side of the building to thermal radiation from the sun.

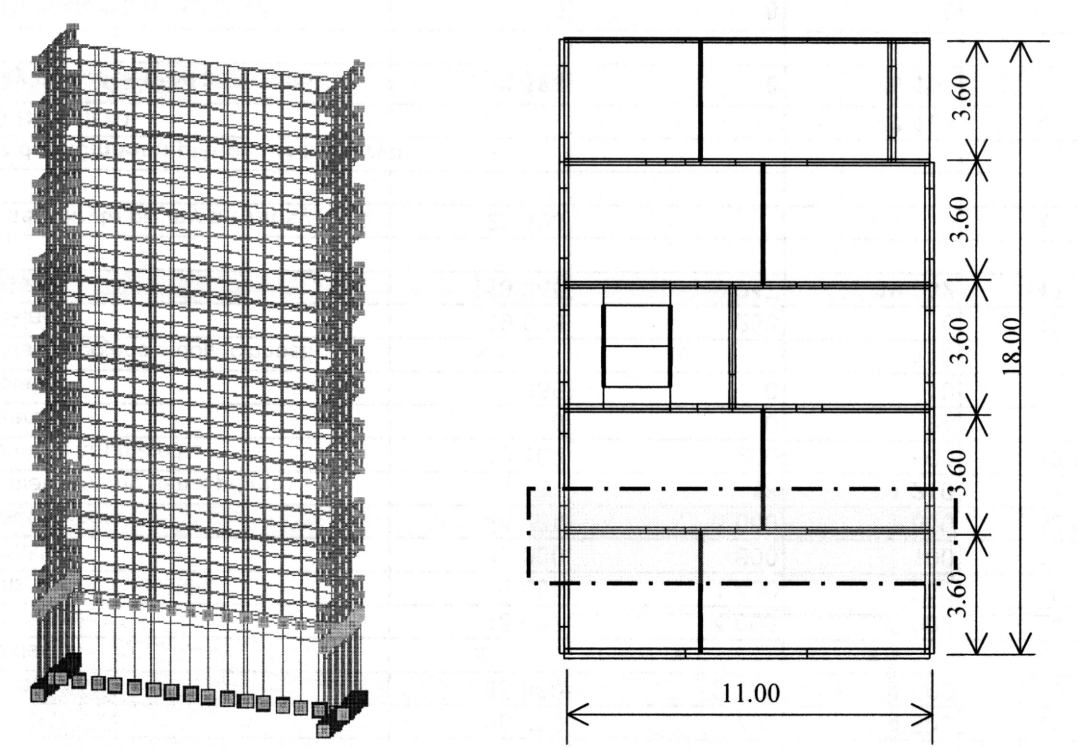

Fig. 7: Ground plan and analyzed part of building G57

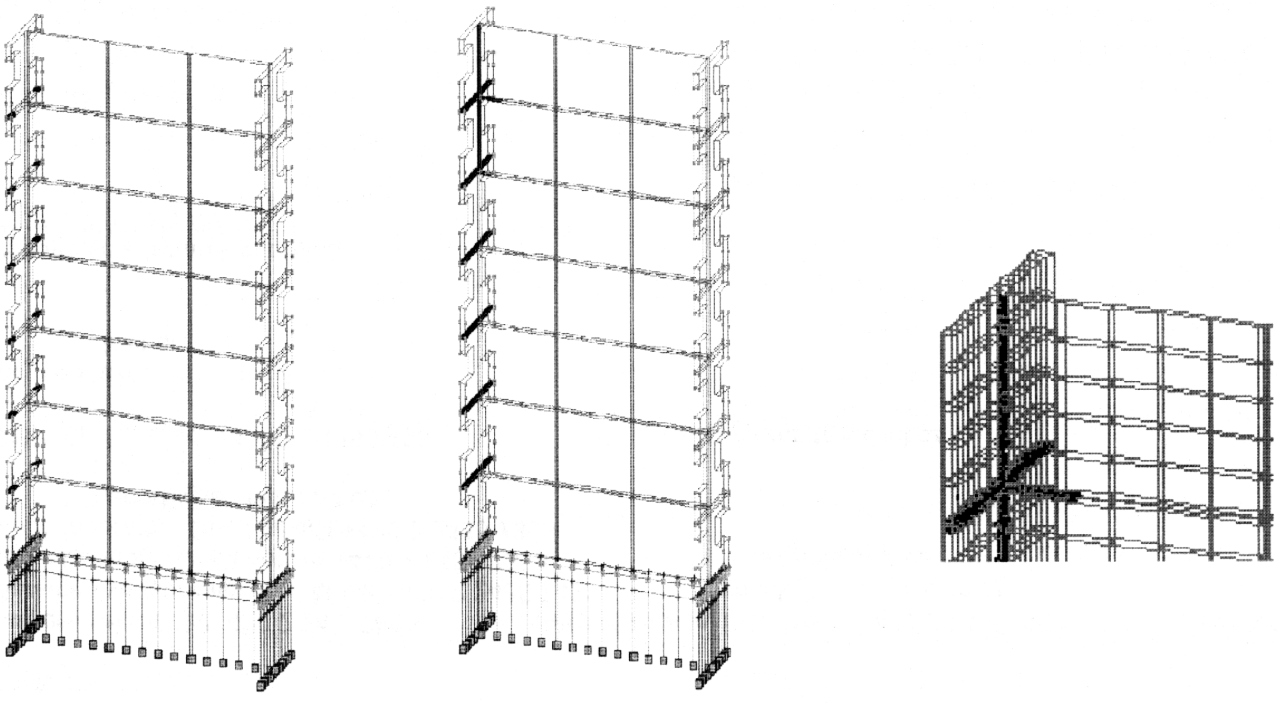

a b c

Fig. 8: Distribution of the failed joints

The maximum value of the temperature change 10 K is considered on the outside surface and conducted to the inner wall (thermal conductivity coefficient λ being 1.43 $Wm^{-1}K^{-1}$).

Table 1: Basic variables

Basic variables		Dimension	Mean
cohesion c		MPa	2.5
friction angle φ		rad	0.52
dead load – material density ρ		kgm^{-3}	2300
loading transferred from ceilings q		kNm^{-2}	6.67
Temperature increments	Δt_1	K	4
	Δt_2	K	4
	Δt_3	K	2

Three temperature levels were used together with the dead load and the loading transferred from the ceilings (Table 1). At the first temperature level ($\Delta t_1 = 4$ K) the values of β attained in the whole structure were greater than 5. At the second level (the total temperature increment $\Delta t = 8$ K) the stiffnesses in the regions of joints with $\beta < 1.5$ were reduced to their residual values and the procedure was repeated. In this example, 10 % of the initial stiffness K_{in} has been chosen for the residual stiffness K_{res}, even though this value somewhat overestimates the values obtained experimentally [5]. The vertical joints in precast buildings of this type are not equipped with reinforcing bars. Their stiffness is assured by the ceiling panels, which overlap the vertical fissures between the wall panels. The resulting distribution of the failed joints is drawn in Fig. 8a (solid lines). The third temperature level (total increment $\Delta t = 10$ K) caused the failure distribution demonstrated in Fig. 8b. The detailed distribution of the deteriorated regions at the top of the building is displayed in Fig. 8c.

When comparing the results obtained in this way with a deterministic non-linear solution by the 2D FEM mentioned in Section 3, nearly the same images of deteriorated regions of joints were reached. It should be pointed out that the two images become different when the coefficient of variation increases.

6 Conclusion

This paper discusses a model describing the failure of a precast construction with random properties of joints and loading by means of index β. It is evident that introducing the residual stiffnesses in joints with $\beta < 1.5$ leads to results that are comparable with the deterministic solution, providing the failure condition is of an adequate type. It appears that the results are almost the same when the level of index β used to reduce the individual stiffnesses varies from 1 to 2. Nevertheless, a fully probabilistic approach, using for example the Monte Carlo method, especially in conjunction with the response surface method, will provide more complex information about the construction behaviour and its reliability.

Acknowledgments

The financial support was provided by GAČR 103/99/0944 and by research project J04/98:210000001.

References

[1] Bittnar, Z., Šejnoha, J.: *Numerical Methods in Structural Mechanics*. ASCE Press, New York, Thomas Telford, London, 1996

[2] Blažek, V., Fajman, P., Šejnoha, J.: *Východiska nelineární analýzy konstrukcí panelových budov* (*Theoretical background of nonlinear analysis of precast structures*). Beton a zdivo (v tisku)

[3] Ducháček, J.: *Nauka o pružnosti a pevnosti II* (*Theory of elasticity II*). SNTL Praha, 1964

[4] Chen, W., F.: *Plasticity in Reinforced Concrete*. McGraw-Hill, New York, 1982

[5] Pume, D.: *Structural Models of Joints between Concrete Wall Elements*. CTU Report, No. 2/1997

[6] *STRUREL, Theoretical Manual*. RCP Consult, München, 1996

Ing. Marie Kalousková, CSc.
phone: +420 2 2435 4489
e-mail: kalousko@fsv.cvut.cz

Ing. Eva Novotná
phone: +420 2 2435 4483
e-mail: novotnae@fsv.cvut.cz

Prof. Ing. Jiří Šejnoha, DrSc.
phone: +420 2 2435 4492
e-mail: sejnoha@fsv.cvut.cz

Dept. of Structural Mechanics
Czech Technical University in Prague
Faculty of Civil Engineering
Thákurova 7, 166 29 Praha 6, Czech Republic

